

T.R. Deberdeev, A.I. Akhmetshina*, L.K. Karimova, S.V. Grishin, D.V. Kochemasova

Kazan National Research Technological University, Kazan, Russia

(*Corresponding author's e-mail: aai-89@mail.ru)

Thermal Behavior of Novel Aromatic Oligoesters and Oligoesteramides

Liquid crystalline polymers, depending on their structure and macromolecular architecture, are found in a number of commercial applications, ranging from state-of-the-art engineering plastics to soft matter artificial muscles and microrobots. Rigid chain liquid crystalline polymers are known as indispensable materials for high technology industries. However, their relatively high costs provoke the search for novel cost-effective mesogenic monomers. In this regard, a series of aromatic oligoesters and oligoesteramides were synthesized via high-temperature polycondensation of aromatic dicarboxylic acids with 4-hydroxybenzoic acid (or 4-aminobenzoic acid) and 1,5-naphthalene diol. The structure of the synthesized compounds was identified using FTIR spectra analysis. According to polarizing microscopy observations, novel oligoester based on 4-hydroxybenzoic acid, 1,5-naphthalene diol and terephthalic acid demonstrated liquid crystallinity with nematic texture, whereas other samples occurred in amorphous state in case of oligoester or in crystalline state in case of oligoesteramides. A relatively wide range of mesophase existence from 120 to 290 °C was found for the thermotropic oligoester using differential scanning calorimetry. While aromatic oligoesters at the beginning of the degradation processes were highly stable towards heat with comparable values of T10, which were equal to 372–378 °C, aromatic oligoesteramides started to decompose at the temperatures lower by more than 50 °C than those for oligoesters.

Keywords: liquid crystalline polymers, phase transitions, polarizing microscopy, thermal stability, solubility, high-temperature polycondensation.

Introduction

Liquid crystals (LCs) are substances that exhibit some degree of order along with fluidity all at once. Depending on the conditions of liquid crystal formation, those substances can be subdivided into thermotropic and lyotropic [1–3]. The first ones undergo a transition from a crystal phase to a mesophase under heating, while the lyotropic LCs are formed in a solution in a certain concentration range. According to the arrangement of molecules in space, the following types of LCs may be differentiated, namely nematic phase, smectic phase, cholesteric phase, and discoid column phase [4].

High-molecular compounds can also demonstrate liquid crystallinity in case of rigid-rod macromolecules. Most examples reported in the literature vary in the position of the liquid crystalline unit and can be divided into the main chain type, side chain type, composite main side chain type, bowl type, star shape, net shape, and shell type. The main-chain thermotropic polymers are advanced materials, which have recently gained considerable attention for high-tech products, such as high-precision, thin-walled electronic components [5–10].

It is necessary to mention that despite their extraordinary properties, e.g., high thermal stability, low thermal expansion, outstanding mechanical properties, chemical resistance and so on, the first representatives of liquid crystalline polymers (poly-4-hydroxybenzoate, poly(1,4-phenylene terephthalamide) faced challenges of intractability and poor processability [11].

Several approaches have been developed to improve the processability of LC polymers (LCP). One implied disruption of chains' regularity by inserting bulky groups of spacers into the macromolecules. Another method is to combine various mesogenic monomers with different length (p-phenyl, p-biphenyl, p-triphenyl, naphthalene moieties) along the chain direction thereof partially excluding intermolecular interactions between the polar linking groups [12]. As such, industrially produced thermotropic LCPs consist of para-linked aromatic monomers and one mesogenic monomer with enlarged length. Vectra A950, which is copolyester composed of HBA and 2,6-hydroxynaphthoic acid, is a striking example of the aforementioned approach. Addition of 6-hydroxy-2-naphthoic acid into the regular chain of poly-4-hydroxybenzoate makes the polymer tractable and processable [12]. Copolymerization of 4-hydroxybenzoic acid with p-phenylene-2,6-dicarboxylate reduces the melting point to 325 °C [12].

On the other hand, incorporation of the amide group into the polymer chain results in enhanced intermolecular interaction and, therefore, makes such polymers preferably lyotropic. In some cases, aromatic polyesteramides maintain their thermotropicity and are molded by traditional methods of plastic processing. Commercially available thermotropic polyesteramide Vectra B950 is made of 2,6-hydroxynaphthoic acid, *p*-hydroxyl acetanilide, and terephthalic acid [13].

Preceding commercialization, scientific research has established that among other isomers, it is 2,6-substituted naphthalene derivatives ensure the stability of the mesophase in a wide temperature range and an acceptable processing temperature [14]. However, it should be mentioned that the cost of this monomer is high and enlarges the cost of the final product.

1,5-substituted naphthalene based LC compounds are also capable to form a mesophase, but in a narrower temperature range than those based on the 2,6-substituted monomer [14]. According to [14], aromatic polyester composed of 4-hydroxybenzoic acid (HBA), terephthalic acid and 1,5-dihydroxynaphthalene residues at any molar ratio of the initial components melts at temperatures above 290 °C, and its mesomorphic properties are poorly researched.

It is worth noting that incorporation of this monomer into the LCPs reduces the cost of the final product by 30–50 % compared to the case of 6-hydroxy-2-naphthoic acid.

Herein, 1,5-naphthalene diol-based aromatic oligoesters and oligoesteramides were selected as possible objects, being able to form a mesophase; their thermal and optical properties were investigated to reveal the liquid crystallinity.

Experimental

4-Hydroxybenzoic acid (4-HBA, 99 %), 4-aminobenzoic acid (4-ABA, 99 %), terephthalic acid (TA, 98 %), isophthalic acid (IA, 99 %), 1,5-dihydroxynaphthalene (DHN, 97 %) were purchased from Sigma-Aldrich. Ditolylmethane (reagent grade) and titanium tetrabutoxide (97 %) were supplied from Angara-reaktiv. Isopropyl alcohol (98 %) was obtained from LLC Chimmed.

The phenyl esters (PE) of corresponding carboxylic acids were synthesized by the reaction of equimolar amount of phenol and carboxylic acid (TA, IA, 4-ABA, 4-HBA). The copolyester was obtained in one stage: a calculated amount of raw materials (the molar ratio of [4-HBA]:[PE of dicarboxylic acid]:[aromatic diol] = 1:1:1) and the catalyst (1 wt%) were added to the 500 mL three-necked round-bottom flask and mixed with 300 ml of ditolylmethane (Table 1, Figure 1). The reaction mixture was heated rapidly up to 200–250 °C with stirring under the nitrogen steam, following the evolution of the calculated amount of phenol+water mixture. The reaction was quenched after reaching the desired amount of side-products.

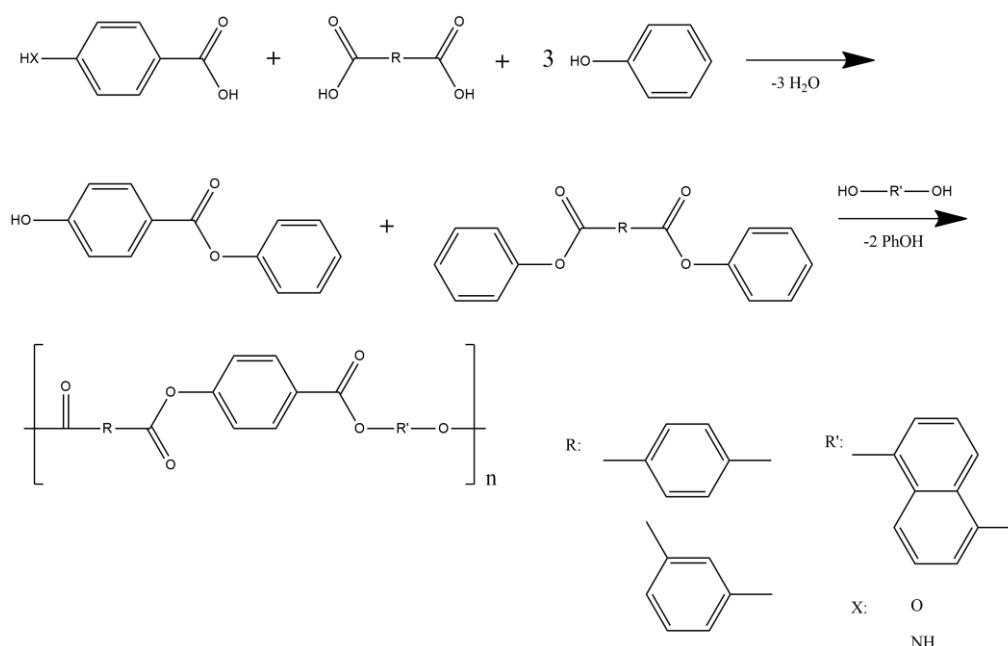


Figure 1. Synthetic route of the aromatic oligoesters and oligoesteramides

General properties of the aromatic oligoesters

LCP	The ratio of monomers	T _g [°C]	T _m [°C]	T _i [°C]	LC Phase
S-1	[4-HBA]:[IA]:[DHN] = 1:1:1	104	–	–	–
S-2	[4-HBA]:[TA]:[DHN] = 1:1:1	–	120	290	Nematic
S-3	[4-ABA]:[IA]:[DHN] = 1:1:1	–	–	–	–
S-4	[4-ABA]:[TA]:[DHN] = 1:1:1	–	307	–	–

The FTIR spectra of the products were recorded on an InfraLUM FT 08 Fourier transform spectrometer using the attenuated total reflection technique. The spectral resolution was 4 cm⁻¹, and the number of scans was 60.

Differential scanning calorimetry (DSC) measurements and thermogravimetric analysis were performed using thermal analyzer TGA/DSC 3+ (Mettler Toledo). The samples (0.1 g) were loaded in alumina pans and ramped to 773 K at a heating rate of 5 K/min in a nitrogen atmosphere.

Optical observation was carried out using the Polam P-312 polarizing microscope equipped with a heating stage in the temperature range of 25–300 °C.

Results and Discussion

Aromatic polyesters and polyesteramides were synthesized via a two-step condensation procedure as described previously. All polymers were obtained in high yields after the precipitation in non-solvent.

Since all used carboxylic acids exhibit approximately equal pK_a values, we expected their similar reactivity and, therefore, the incorporation of these monomers into macromolecules. Indeed, the results of FTIR spectroscopy revealed this assumption and the IR spectra demonstrated embedding of all raw materials into the polymeric chains.

Figure 2 depicts the FTIR graph of the polymeric samples and their characteristic bands. Ones ($\nu_{C=C}$) for the C=C stretching vibrations of aromatic (benzene and naphthalene) rings were found at 1450–1624 cm⁻¹. The peak located at 1740 cm⁻¹ is assigned to the C=O group stretching. Besides, the OH in-plane bending vibrations for end-groups may be found as low-intensity band at 1455 cm⁻¹. The IR band with a mild intensity at 1257 cm⁻¹ is originated by the C(Ar)-O bond presence. Moreover, the peaks that appeared at 1257 and 1057 cm⁻¹ are attributed to asymmetrical and symmetrical stretching of the C-O-C group. The C-H bending vibrations in oligoesters were observed at 750–900 cm⁻¹.

For the synthesized polyesteramides, the amide I band was resolved into two bands at about 1681 cm⁻¹ (a “free” carbonyl group) and 1651 cm⁻¹ (a hydrogen-bonded carbonyl group). The intensive shoulder at 1530–1550 cm⁻¹ is attributed to NH deformation vibrations, as well as the peak at 1507 is assigned to N-H bending vibrations. The C-C stretching vibrations in the aromatic ring remain unchanged compared to aromatic polyesters. The stretching vibrations of the C-O-C group in S-3 and S-4 is observed at 1250 cm⁻¹ and 1270 cm⁻¹, respectively.

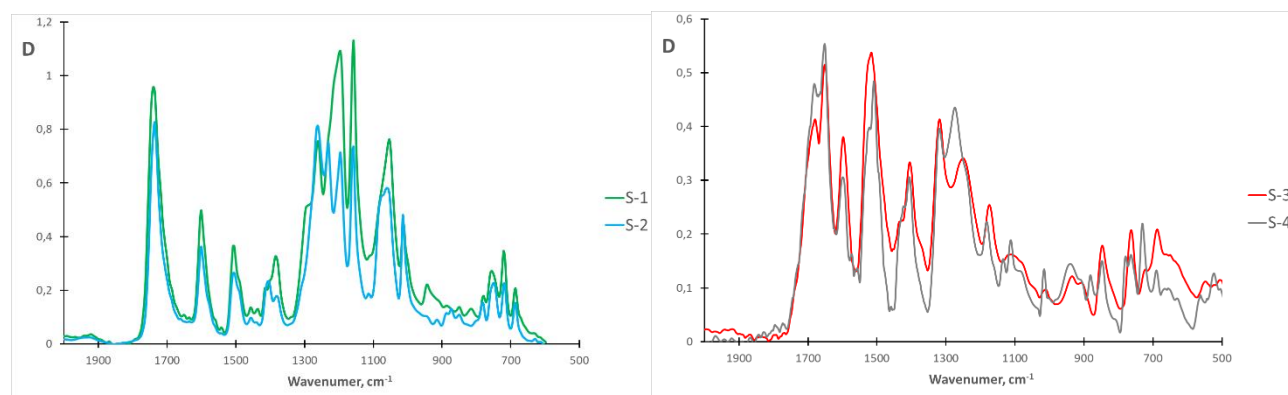


Figure 2. FTIR spectra of aromatic polyesters and polyesteramides

Hot-stage polarized optical microscopy (POM) was performed to observe the LC behavior of the polymeric samples. Among the synthesized compounds, the oligoester S-2 solely demonstrated the presence of a

nematic texture in a temperature range from 120 to 290 °C. Whereas the recent reports have claimed about instability of mesophase, which is formed by low-molecular LCs containing the residue of 1,5-naphthalene diol. The present work shows the opposite trend. Aromatic polyester S-2 tends to form a stable nematic phase with a wide processing window. When a linear configuration of TA is completely replaced by a bent-core geometry of IA, the polyester S-1 loses the ability to form a LC phase. Therefore, the images of POM show only the isotropic melt, appearing after the glass transition temperature. In case of polyesteramides, S-3 and S-4, those samples were intractable up to 290 °C, limited by an upper temperature bound of the microscope.

The phase transitions in the samples were confirmed using differential scanning calorimetry. From DSC data, it was evident that introduction of IA into the linear aromatic chain resulted in an absence of a mesophase. No endothermic peaks for this sample attributed to melting of the crystalline phase or isotropization were found on the thermograms (Figure 3).

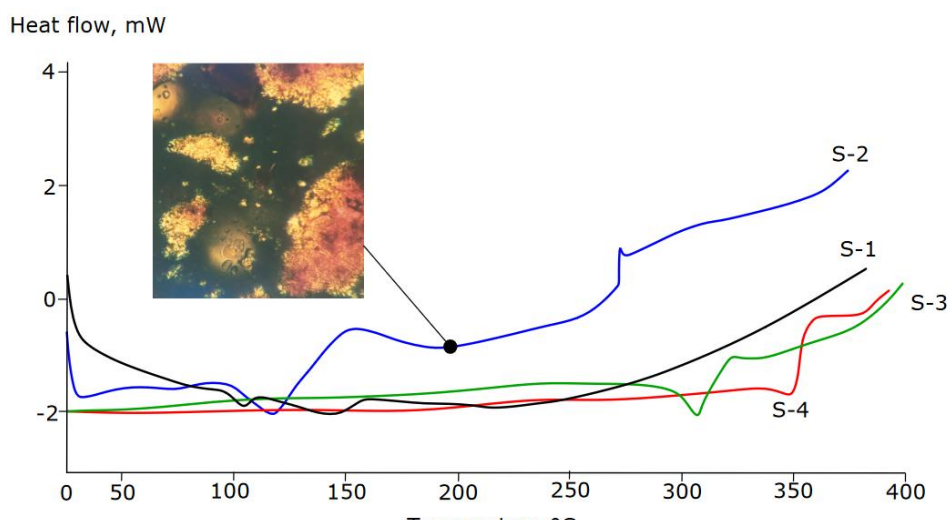


Figure 3. DSC scans of the samples

Figure 3 illustrates that the polymer S-2 clearly undergoes a phase transition and forms a mesophase at 120 °C with subsequent melting at 270 °C. Those data are consistent with results obtained from the optical microscopy. Upon introducing of 4-ABA instead of 4-HBA, polyesteramides have no accessible melting point and maintain intractability up to thermal decomposition temperatures. However, in case of S-4, one endopeak at 307 °C probably corresponding to the melting process was detected.

Some representatives of aromatic polyesteramides are recognized as thermotropic LCs; others are structured in an ordered state, only being dissolved in harsh conditions of aggressive solvents. To estimate the processability of the samples through solution casting, we have calculated the solubility parameter of the polymers using a group contribution method [15].

Solubility parameter δ is closely related to the cohesive energy according to the following equation:

$$\delta = \left(\frac{E_{coh}}{V} \right)^{1/2},$$

where E_{coh} is the cohesive energy (cal/mol), V is the molar volume (\AA^3).

Group contributions to E_{coh} and V are represented in the aforementioned reference. As can be concluded from the solubility parameter calculations, aromatic oligoesters and oligoesteramides dissolve presumably in amide solvents ($\delta_{\text{DMSO}} = 12.93$, $\delta_{\text{DMF}} = 12.14$) (Table 2).

Qualitative tests of the solubility in DMSO and DMF revealed that both oligoesters were completely soluble, whereas the close packing through hydrogen bonds between amide groups resulted in reduced solubility of S-3 and S-4. Oligoesteramides were soluble in concentrated H_2SO_4 and it made possible to form a lyotropic phase only under harsh conditions.

Cohesive energy and solubility parameters of the samples

Samples	E_{coh} , kcal/mol	V , Å ³	δ , (cal/cm ³) ^{0.5}
S-1	24.351	357.0	10.61
S-2	24.351	357.0	10.61
S-3	29.343	360.9	11.58
S-4	29.393	352.5	11.72
DMSO	–	–	12.93
DMF	–	–	12.14

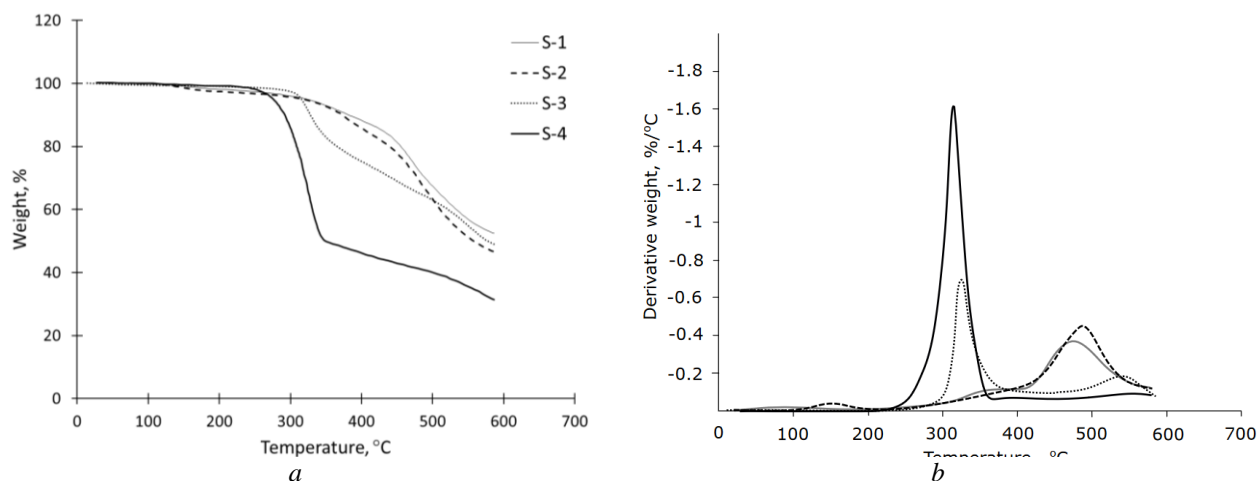


Figure 4. TGA and DTG curves of the samples

To study the thermal decomposition of the polymers, thermogravimetric analysis was performed between 25–600 °C in flowing N₂ at a heating rate of 10 °C/min. Figure 4a depicts the TGA curves for experiments with oligoesters and oligoesteramides. Figure 4b represents the curves plotting the first derivative of TGA thermograms. Noteworthy is that the thermal stability of oligoesters exceeded that for oligoesteramides. The weight loss percentages are close at different heating rates for S-1 and S-2. The temperature for 10 % gravimetric loss ($T_{10\%}$), which is the key indicator for thermal stability, was in the range of 372–378 °C for oligoesters and 291–326 °C for oligoesteramides, respectively. The temperatures at 10 % weight loss percentages and the temperature of maximal rate of the weight loss T_{dm} are listed in Table 3, from which it can be seen that the order of thermal stability is S-1 > S-2 > S-3 > S-4 in N₂. Most probably, the lowering of thermal stability in case of oligoesteramides is closely related to the fact that the average bond dissociation energy of C-N (about 73 kcal/mol) is smaller than that of C-O (approximately 85 kcal/mol). Therefore, the introduction of amide bonds into the structure makes S-3 and S-4 less thermally stable than S-1 and S-2.

It was established (Figure 4b) that the major decomposition of the oligoesters occurred in the temperature range from 250 to 350 °C. The highest rates of thermal decomposition for oligoesteramides were achieved in a range of 420–500 °C. Therefore, the kinetic parameters of thermal decomposition were evaluated only for the major decomposition range. The kinetic parameters were calculated using Coats-Redfern method [16]:

$$\ln \left[\frac{-\ln(1-\alpha)}{T^2} \right] = \ln \frac{AR}{\beta E_a} - \frac{E_a}{RT},$$

where α is fraction of decomposition, E_a is the activation energy, A is the pre-exponential factor, R is the universal gas constant, β is the heating rate.

Plotting $\ln \left[\frac{-\ln(1-\alpha)}{T^2} \right]$ against $1/T$ should give a straight line with a slope proportional to the activation energy ($-E_a/R$). Figure 5 demonstrates the Coats-Redfern plots of the decomposition step for the sam-

ples. The coefficient of correlation (R^2) is obtained by plotting $\ln \left[\frac{-\ln(1-\alpha)}{T^2} \right]$ versus $(1/T)$ using a linear approximation function. The relatively high values of R^2 offer an ability of the proposed model to fit the experimental TGA data.

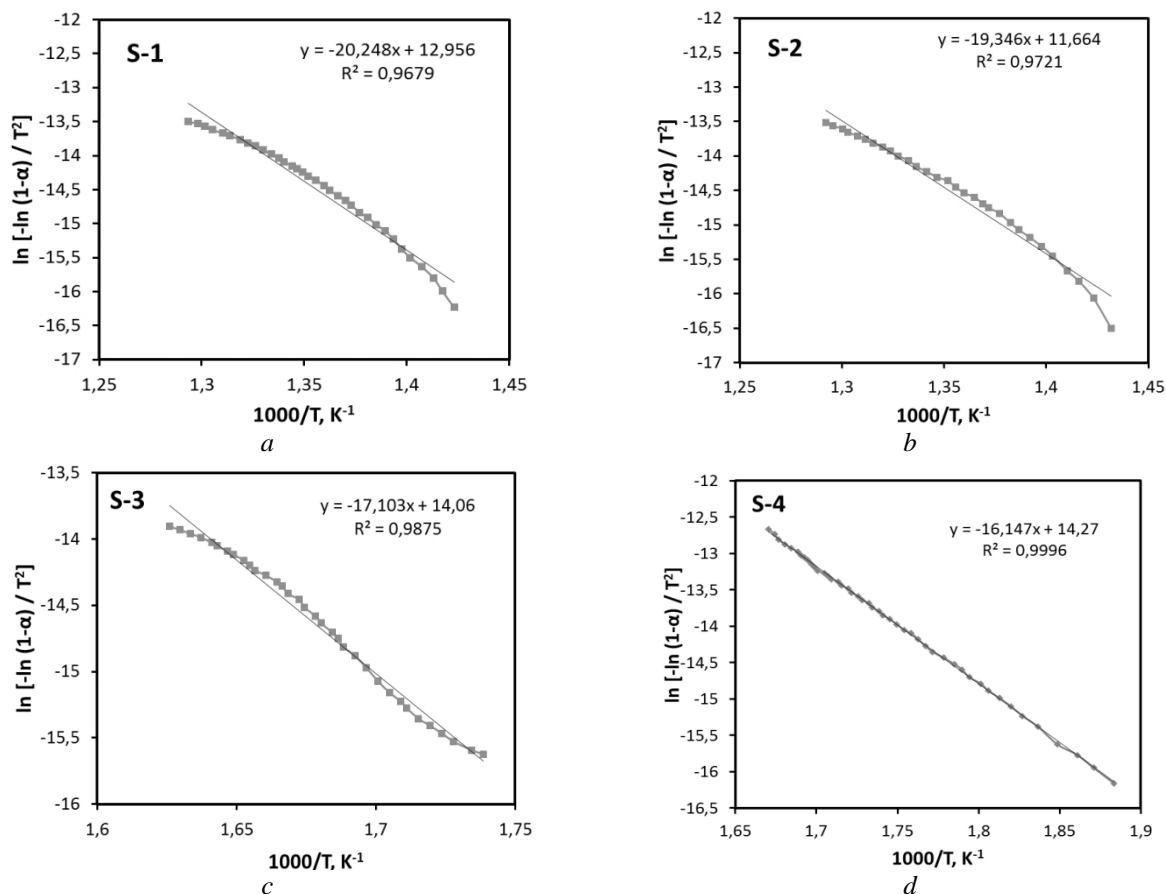


Figure 5. Coats-Redfern plots for the samples

Table 3 presents the results of the calculated activation energies for each sample. It is clear that the results highly correlated with the Coats-Redfern model since R^2 values exceeded 0.9. The activation energy of thermal decomposition of oligoester S-2 was $161.10 \text{ kJ mol}^{-1}$, slightly less than that ($168.35 \text{ kJ mol}^{-1}$) of oligoester S-1. The E_a was found to be $142.20 \text{ kJ mol}^{-1}$ and $134.25 \text{ kJ mol}^{-1}$ for oligoesteramides S-3 and S-4. In general, the findings of a kinetic study were in consistent with the thermal behavior of the samples given above. A relatively weak bond dissociation energy of oligoesteramides contributed to loosening of stability.

Table 3

Results of TGA analysis of the samples

Samples	$T_{10}, ^\circ\text{C}$	$T_{dm}, ^\circ\text{C}$	Residue, %	$E_a, \text{kJ/mol}$
S-1	378	464	52.5	168.35
S-2	372	494	46.6	161.10
S-3	326	325	48.8	142.20
S-4	291	323	31.3	134.25
Vectra A950 [19]	503	–	–	232.04
Vectra B950 [19]	502	–	–	196.71

The TGA results are different from the ones for the commercially available polyesters Vectra A650 and Vectra B950, as shown in Table 3. The explanation given for this large variance is related to a molecular

weight of the samples. The synthesized samples are noticeably inferior in terms of thermal stability, which can depend both on the chemical structure of oligoesters or oligoesteramides and on the content of end groups. Faster degradation of oligomers, most probably, is associated with the relatively low molecular weight of the samples [17] and the increased content of end groups, which are the first to be involved in the thermal degradation process [18]. However, due to the samples contain reactive end groups, the heat treatment of the samples, accompanied by post-polycondensation, is expected to improve their thermal stability.

Conclusions

In this work, we synthesized and characterized the mesomorphic and thermal behavior of aromatic oligoesters and oligoesteramides containing the 1,5-naphtalene moiety. DSC experiments revealed the existence of a phase transition in the temperature range of 120–290 °C in case of oligoester based on 4-hydroxybenzoic acid, 1,5-naphtalene diol, and terephthalic acid. Study of phase transitions using polarized light microscopy evidenced an optical activity of the sample and formation of a mesophase with a nematic texture. Replacement of linear terephthalic acid with kinked isophthalic acid resulted in an amorphous nature of the synthesized oligoester. Oligoesteramides showed no phase transitions associated with existing of a mesophase. Since those samples had been slightly soluble in amide solvents, but completely dissolved in sulfuric acid, they were presumptively capable of ordering in a lyotropic liquid crystalline phase. Aromatic oligoesters possessed higher thermal stability among polymeric samples and similar values of the 10 % weight loss temperature at 372–378 °C.

References

- 1 Shibaev, V.P. (2014). Liquid-crystalline polymer systems: From the past to the present. *Polymer Science Series A*, 56(6), 727–762. <https://www.doi.org/10.1134/S0965545X14060091>
- 2 Deberdeev, T.R., Akhmetshina, A.I., Karimova, L.K., Ignat'eva, E.K., Deberdeev, R.Ya., & Berlin, A.A. (2020). Heat-Resistant Polymer Materials Based on Liquid Crystal Compounds. *Polymer Science, Series C*, 62(2), 145–164. <https://doi.org/10.1134/s1811238220020034>
- 3 Ohm, C, Brehmer, M, & Zentel, R. (2010). Liquid Crystalline Elastomers as Actuators and Sensors. *Advanced Materials*, 22(31), 3366–3387. <https://doi.org/10.1002/adma.200904059>
- 4 Donnio, B. (2014). Liquid-crystalline metallodendrimers. *Inorganica Chimica Acta*, 409, 53–67. <https://doi.org/10.1016/j.ica.2013.07.045>
- 5 Ji, Y., Bai, Y., Liu, X., & Jia, K. (2020). Progress of liquid crystal polyester (LCP) for 5G application. *Advanced Industrial and Engineering Polymer Research*, 3(4), 160–174. <https://doi.org/10.1016/j.aiepr.2020.10.005>
- 6 Wang, L., & Li, Q. (2016). Stimuli-Directing Self-Organized 3D Liquid-Crystalline Nanostructures: From Materials Design to Photonic Applications. *Advanced Functional Materials*, 26(1), 10–28. <https://doi.org/10.1002/adfm.201502071>
- 7 Gantenbein, S., Masania, K., Woigk, W., Sesseg, J.P.W., Tervoort, T.A., & Studart, A.R. (2018). Three-dimensional printing of hierarchical liquid-crystal-polymer structures. *Nature*, 561(7722), 226–230. <https://doi.org/10.1038/s41586-018-0474-7>
- 8 Kato, T., Uchida, J., Ichikawa, T., & Soberats B. (2018). Functional liquid-crystalline polymers and supramolecular liquid crystals. *Polymer Journal*, 50(1), 149–166. <https://doi.org/10.1038/pj.2017.55>
- 9 Zhang, Y., Wang, Z., Yang, Y., Chen, Q., Qian, X., Wu, Y., Liang, H., Xu, Y., Wei, Y., & Ji, Y. (2020). Seamless multimaterial 3D liquid-crystalline elastomer actuators for next-generation entirely soft robots. *Science Advances*, 6(9). <https://doi.org/10.1126/sciadv.aay8606>
- 10 Chen, T., Han, J.Y., Okonski, D.A., Kazerooni, D., Ju, L., & Baird, D.G. (2021). Thermotropic liquid crystalline polymer reinforced polyamide composite for fused filament fabrication. *Additive Manufacturing*, 40, 101931. <https://doi.org/10.1016/j.addma.2021.101931>
- 11 Thakur, V.K., & Kessler, M.R. (2015). *Liquid Crystalline Polymers Volume 2-Processing and Applications*. Heidelberg: Springer Cham. <https://doi.org/10.1007/978-3-319-20270-9>
- 12 Jackson, W.J., & Kuhfuss, H.F. (1976) Liquid crystal polymers. I. Preparation and properties of p-hydroxybenzoic acid copolyesters. *Journal of Polymer Science: Polymer Chemistry Edition*, 14(8), 2043–2058. <https://doi.org/10.1002/pol.1976.170140820>
- 13 Han, J.Y., Chen, T., Mu, Q., & Baird, D.G. (2021). Thermotropic liquid crystalline polymer reinforced polypropylene composites enhanced with carbon nanotubes for use in fused filament fabrication. *Polymer Composites*, 42(8), 4115–4127. <https://doi.org/10.1002/pc.26134>
- 14 Jackson, W.J. (1983). Liquid crystalline polymers. 5. Liquid crystalline polyesters containing naphthalene rings. *Macromolecules*, 16(7), 1027–1033. <https://doi.org/10.1021/ma00241a001>
- 15 Askadskii, A.A. (2003). *Computational Materials Science of Polymers*. Cambridge: Cambridge international science publishing. [https://doi.org/10.1016/s1369-7021\(03\)00438-3](https://doi.org/10.1016/s1369-7021(03)00438-3)

16 Coats, A.W., & Redfern, J.P. (1964). Determination of kinetic parameters from thermogravimetric data. *Thermochimica Acta*, 24 (1), 182–185. [https://doi.org/10.1016/0040-6031\(78\)85150-8](https://doi.org/10.1016/0040-6031(78)85150-8)

17 Chrissafis, K., Paraskevopoulos, K.M., & Bikiaris, D.N. (2006). Effect of molecular weight on thermal degradation mechanism of the biodegradable polyester poly(ethylene succinate). *Thermochimica Acta*, 440(2), 166–175. <https://doi.org/10.1016/j.tca.2005.11.002>

18 Bosnyak, C.P., Knight, G.J., & Wright, W.W. (1981). Thermal stability of some aromatic polyesters and poly(ester carbonates). *Polymer Degradation and Stability*, 3(4), 273–283. [https://doi.org/10.1016/0141-3910\(81\)90023-9](https://doi.org/10.1016/0141-3910(81)90023-9)

19 Jin, X., & Chung, T.-S. (1999). Thermal decomposition behavior of main-chain thermotropic liquid crystalline polymers, Vectra A-950, B-950, and Xydar SRT-900. *Journal of Applied Polymer Science*, 73(11), 2195–2207. [https://doi.org/10.1002/\(sici\)1097-4628\(19990912\)73:11<2195::aid-app17>3.0.co;2-3](https://doi.org/10.1002/(sici)1097-4628(19990912)73:11<2195::aid-app17>3.0.co;2-3)

Т.Р. Дебердеев, А.И. Ахметшина, Л.К. Каримова, С.В. Гришин, Д.В. Кочемасова

Жаңа ароматты олигоэфирлер мен олиготерамидтердің жылулық қасиеттері

Химиялық құрылымы мен макромолекулярлық құрылысына байланысты сұйық кристалды полимерлер супер құрылымды инженерлік пластиктен бастап жасанды бұлшықеттер мен микророботтарға дейін әртүрлі жоғары технологиялық салаларда қолданылуы мүмкін. Қаттытiзбектi сұйық-кристалды полимерлер жоғары берiктiк қасиеттерi бар ыстыққа төзiмдi материалдар ретiнде кеңiнен тарады. Алайда, олардың айтарлықтай жоғары құны оларды синтездеу үшiн жаңа экономикалық тиiмдi мезогендi мономерлердi iздеуге әкелетiнiн атап өткен жөн. Осыған байланысты осы жұмыста жоғары температурада каталитикалық поликонденсациялау арқылы ароматты дикарбон қышқылдары, 4-гидроксibenзой қышқылы (немесе 4-аминбензой қышқылы) және 1,5-нафталендиол негiзiндегi бiрқатар ароматты олигоэфирлер мен олиготерамидтер синтезделдi. Синтезделген қосылыстардың құрылымы ИК-спектроскопия көмегiмен анықталды. Поляризацияланған оптикалық микроскопия арқылы алынған нәтижелерге сәйкес, 4-гидроксibenзой қышқылы, 1,5-нафталендиол және терефтал қышқылы негiзiндегi жаңа олигоэфир нематикалық құрылымды сұйық кристалды фазаның болуын көрсеттi, ал басқа үлгiлер аморфты күйде (олигоэфир) немесе кристалдық күйде (олиготерамидтер) болды. Термотропты олигоэфир үшiн дифференциалды сканерлеу калориметриясын қолдана отырып, температура интервалы 120-дан 290 °C-қа дейiнгi болып табылатын мезофазаның бар болу диапазоны сипатталды. Ароматты олигоэфирлер ыдырау процестерiнiң басында 372–378 °C-қа тең T10 салыстырмалы мәндерiнде температура әсерiне айтарлықтай жоғары тұрақтылық көрсеттi. Ароматты олиготерамидтер олигоэфирлерге қарағанда 50 °C төмен температурада ыдырай бастады.

Кiлт сөздер: сұйық кристалды полимерлер, фазалық ауысулар, поляризациялық микроскопия, термиялық тұрақтылық, ерiгiштiк, жоғары температурадағы поликонденсация.

Т.Р. Дебердеев, А.И. Ахметшина, Л.К. Каримова, С.В. Гришин, Д.В. Кочемасова

Термические свойства новых ароматических олигоэфиров и олигоэфирамидов

В зависимости от своего химического строения и макромолекулярной архитектуры жидкокристаллические полимеры могут быть применимы в различных высокотехнологичных отраслях, начиная с суперконструкционных инженерных пластиков и завершая искусственными мышцами и микророботами. Жесткоцепные жидкокристаллические полимеры получили распространение в качестве термостойких материалов с высокими прочностными свойствами. Однако стоит отметить, что их достаточно высокая стоимость обуславливает поиск новых экономически более рентабельных мезогенных мономеров для их синтеза. В связи с этим в данной статье синтезирован ряд ароматических олигоэфиров и олигоэфирамидов на основе ароматических дикарбоновых кислот: 4-гидроксibenзойной кислотой (или 4-аминобензойной кислотой) и 1,5-нафталиндиола методом высокотемпературной каталитической поликонденсации. Структуру синтезированных соединений идентифицировали с использованием ИК-спектроскопии. Согласно результатам, полученным методом поляризационной оптической микроскопии, новый олигоэфир на основе 4-гидроксibenзойной кислоты, 1,5-нафталиндиола и терефталевой кислоты проявлял наличие жидкокристаллической фазы с нематической текстурой, тогда как другие образцы находились в аморфном состоянии (олигоэфир) или в кристаллическом состоянии (олигоэфирамиды). С помощью дифференциальной сканирующей калориметрии для термотропного олигоэфира охарактеризован диапазон существования мезофазы, составляющий температурный интервал от 120 до 290 °C. Ароматические олигоэфир в начале процессов деструкции проявляли доста-

точно высокую стабильность к воздействию температуры при сопоставимых значениях T₁₀, равных 372–378 °С, ароматические олигоэфирамиды начинали разлагаться при температурах более чем на 50°С ниже, чем у олигоэфиров.

Ключевые слова: жидкокристаллические полимеры, фазовые переходы, поляризационная микроскопия, термическая стабильность, растворимость, высокотемпературная поликонденсация.

Information about authors*

Deberdeev, Timur Rustamovich — Doctor of Technical Sciences, Chair of Department, Kazan National Research Technological University, Karl Marx street, 68, 420015, Kazan, Russia; e-mail: deberdeev@mail.com; <https://orcid.org/0000-0003-2714-519X>;

Akhmetshina, Alsu Islamovna (*corresponding author*) — Candidate of Chemical Sciences, Associate Professor, Kazan National Research Technological University, Karl Marx street, 68, 420015, Kazan, Russia; e-mail: aai-89@mail.ru; <https://orcid.org/0000-0003-3960-8462>;

Karimova, Liana Katifyanovna — Candidate of Technical Sciences, Associate Professor, Kazan National Research Technological University, Karl Marx street, 68, 420015, Kazan, Russia; e-mail: li-karimova@yandex.ru; <https://orcid.org/0000-0002-3061-296X>;

Grishin, Sergey Vaycheslavovich — PhD student, Kazan National Research Technological University, Karl Marx street, 68, 420015, Kazan, Russia; e-mail: svg95@list.ru;

Kochemasova, Darya Vladimirovna — PhD student, Kazan National Research Technological University, Karl Marx street, 68, 420015, Kazan, Russia; e-mail: d_kochemasova@inbox.ru.

*The author's name is presented in the order: *Last Name, First and Middle Names*